Egyptian Journal of Radiology and Nuclear Medicine

RESEARCH

Open Access

Diagnostic performance of ADC value in histopathological grading of mass-forming cholangiocarcinoma

Heba Said Ellaban[1], Mohamed R. El-Kholy[2], Tarek F. Abdellah[2] and Mohamed Saied Abdelgawad[1*]

Abstract

Background: Various invasive and non-invasive imaging modalities are used to diagnose and stage cholangiocarcinoma (CC). In this study, we aimed to assess the role of diffusion-weighted imaging (DWI) and apparent diffusion coefficient (ADC) value measurement in diagnosing and grading CC with mass formation. The study was conducted on 38 cases, including 24 males and 14 females, with ages ranging from 34 to 77 years with a mean age of 61.52 ± 10.45 year. Patients were referred by the Hepatobiliary Surgery and Hepatology departments of our institution between October 2019 and November 2021. With respect to the patients diagnosed with mass-forming CC by pathology, they underwent dynamic MR 1.5 T. CC was evaluated qualitatively using visual analysis of DW-MR images and quantitatively with measurement of ADC values.

Results: The mean ADC of mass-forming carcinoma was lower than that of hepatic parenchyma and more than that of the splenic parenchyma. Poorly differentiated CC was associated with a lower ADC value (mean 0.98 ± 0.12), while well-differentiated CC was associated with a higher ADC value (mean 1.23 ± 0.16). The cutoff value for poorly differentiated CC ADC measurements was less than 1.15, whereas it was greater than 1.15 for the well-differentiated CC.

Conclusions: DWI is a new effective technique for detecting and improving CC diagnosis as a safe, non-invasive, and non-contrast dependent.

Keywords: MRI, DWI, Cholangiocarcinoma, ADC value

Background

DW-MRI has been used to investigate a variety of malignant hepatic neoplasms. Cholangiocarcinoma (CC) is the liver's most common primary malignant tumor after hepatocellular carcinoma, accounting for 5–30% of all primary hepatic malignant tumors [1, 2].

CC tends to extend between the hepatocytes and along the duct walls and nerves, with approximately 10% of cases being multifocal [3, 4] (Fig. 1).

The American Joint Committee on Cancer (AJCC) and the College of American Pathologists grade bile duct-derived adenocarcinomas (e.g., cc) into four histologic grades: well-differentiated (>95% of tumor composed of glands), moderately differentiated (50–95% of tumor composed of glands), poorly differentiated (5–49% gland formation), and undifferentiated (less than 5% gland formation). Tumor grade is an independent predictor of patient survival and disease recurrence [5].

Various invasive and non-invasive imaging modalities are used to for the diagnose and staging of cholangiocarcinoma. The non-invasive imaging methods include ultrasonography (US), multi-detector computed tomography (MDCT), magnetic resonance imaging (MRI), and positron-emission tomography (PET-CT) [6, 7] (Fig. 2).

*Correspondence: mselgawad@yahoo.com

[1] Radiology Department, National Liver Institute, El-Menofuia University, Shebin Elkoum, Egypt
Full list of author information is available at the end of the article

In terms of different focal liver lesions, DW-MR image analysis can be made quantitatively with ADC measurement and qualitatively with visual analysis of DW-MR images). DW-MRI has been used to study a variety of malignant hepatic tumors. However, a few studies have highlighted the appearance of intrahepatic CC on DW-MRI [7, 8].

Many researchers have suggested that diffusion-weighted (DW) MRI increases the sensitivity of MRI for CC diagnosis and differentiates between intrahepatic CC and other malignant neoplasms [9, 10].

The continuous development and improvement of hardware and software for magnetic resonance imaging (MRI), the use of parallel acquisition techniques to reduce scan time and improve spatial resolution, and the wide application of the shortened echo chain technique in spin-echo echo-planar imaging (SE-EPI), DWI has been increasingly used in a wide range of clinical applications. In recent years, the application of DWI for the diagnosis of numerous conditions has attracted increased interest and been the focus of numerous studies [11].

The aim of this study was to assess the role of diffusion MRI-weighted imaging and ADC measurement in the diagnosis and grading of CC with mass formation.

Methods

This prospective study was conducted on 38 patients; 24 males and 14 females. Their age ranged from 34 to 77 years (Fig. 3).

The patients were collected during the period from October 2019 to November 2021.

Ethical consideration: Consent was obtained from patients or their relatives before performing MRI, and they had the right to refuse at any time. The study was approved by the Research Ethics Committee (Fig. 4).

Inclusion criteria

Tissue histopathology confirmed the existence of CC in patients suffering from mass-forming CC.

Exclusion criteria

The exclusion criteria include patients with poor general condition (e.g., tense ascites) and/or an inability to hold their breath, patients with general contraindications to MRI: ferromagnetic prostheses (aneurysmal clip, surgical clips) or foreign bodies (gunshot pellets), cardiac pacemaker or electronic neurostimulator, claustrophobia, or unstable clinical status and contraindications to contrast media administration: history of prior allergic-type reaction to gadolinium chelates or severe renal insufficiency.

Procedure

Before the procedure, all patients in this study fasted for eight hours. A venous catheter was placed in a peripheral vein (antecubital vein in most cases), passing through a long connecting tube to an automatic injector to allow easy injection. The patient was instructed on breathing-hold techniques. MR imaging was performed on a high field system (GE-1.5 Tesla—general electric optima 450w, 32 channels) using a phased array coil to cover the whole liver.

MR protocol used Coronal Survey BFFE, Axial T1-weighted (T1WI) images (FRFSE/PROP): Axial in-phase and out-phase gradient echo sequence (dual-FFE-BHSENSE) axial images: Axial T2-weighted (ax T2 RTr prop), Coronal T2W-(FRFSE/PROSP), Axial T2 fat suppression sequence, Axial heavy T2-weighted images. Diffusion study (DW): Respiratory-triggered fat-suppressed single-shot echo-planar DW imaging was performed in the transverse plane with tri-directional diffusion gradients using b values 0.500 and 1200 s/mm^2 to increase sensitivity to cellular packing. Dynamic study: Dynamic study was performed after bolus injection of 0.1 mmol/kg body weight of Gd-DTPA at a rate of 2 ml/s, flushed with 20 ml of sterile 0.9% saline solution from the antecubital vein. Patients were asked to hold their breath at the end of expiration.

Imaging evaluation: Data analysis was performed in collaboration with two radiology consultants with experience of 3 and 10 years in abdominal MRI imaging at the workstation. All imaging evaluations began with the morphological features of the mass-forming CC. Imaging evaluation was performed by reviewing the associated radiological examinations rather than MRI. The morphological features of the mass-forming CC were recorded (such as shape, site, size, margin, signal characteristics, liver capsule, enhancement pattern, and vascular invasion). The mass-forming type was diagnosed based on its characteristic enhancement pattern during the dynamic phase (early arterial enhancement with delayed filling in a pattern of enhancement) together with a histopathological study.

All lesions were larger than 2 cm, so measuring the ADC value of mass forming was done by drawing one circular ROI covering as much of the lesion's interior volume as possible. ROIs were placed to include almost the area of the homogeneous solid portion of CC, avoiding the lesions' peripheral parts to exclude partial volume effects of adjacent extra-lesional tissue.

The ADC value of the normal liver parenchyma was measured by drawing ROI at a fixed site such as segment IV.

The ADC value of splenic parenchyma was measured by drawing the ROI at its middle region.

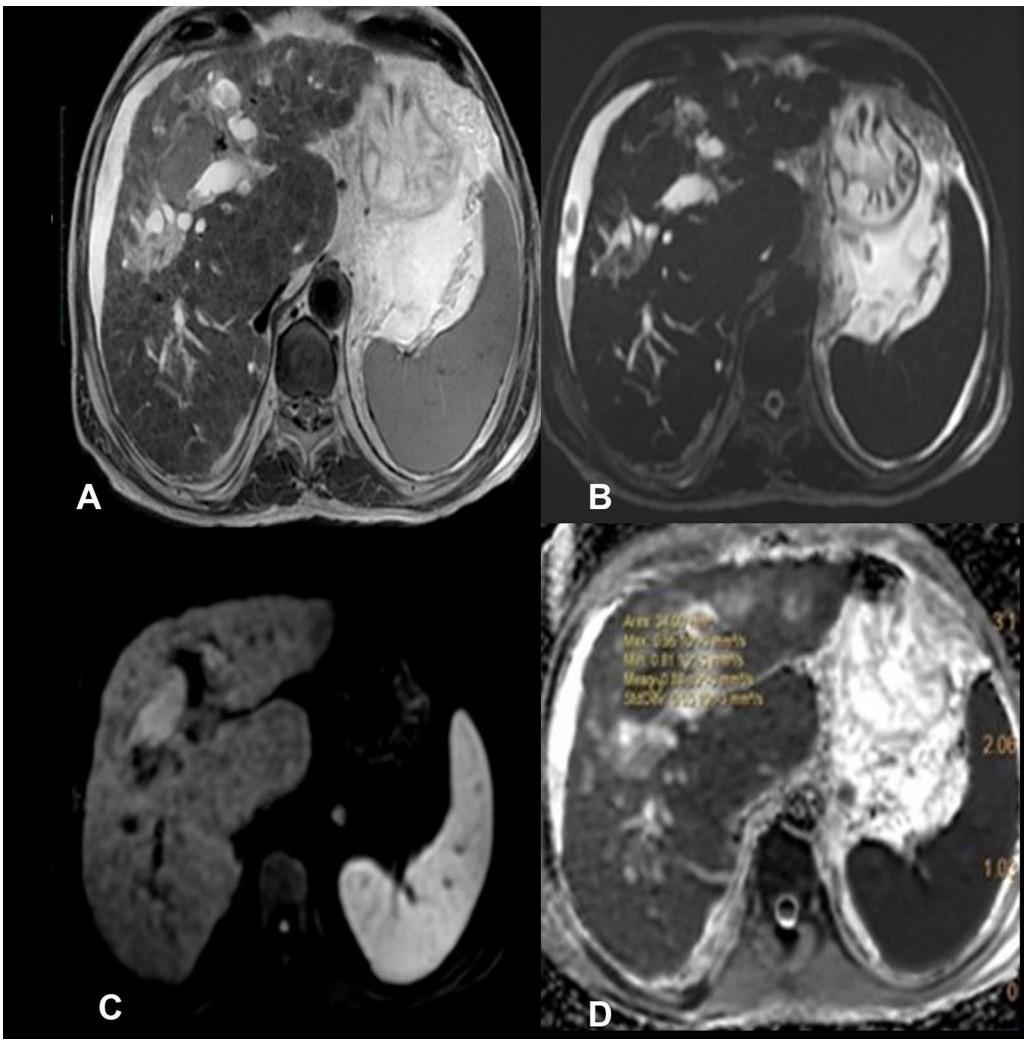

Fig. 1 A 65-year-old male patient with high-grade CC **A** Axial T2WI shows an intermediate signal intensity lesion in segment IV of the left hepatic lobe. Minimal perihepatic ascites is noted. **B** Axial MRCP shows moderate biliary radicles dilatation. **C** The lesion displays high signal intensity on DWI (restricted diffusion). **D** ADC value of the lesion is (0.9×10^{-3} mm^2/s)

Finally, we compared the different mass-forming CC mean ADC values with the degree of tumor differentiation by histopathology results.

Statistical analysis: Data were fed to the computer and analyzed using IBM SPSS software package version 20.0 (Armonk, NY: IBM Corp), including descriptive: (e.g., percentage (%), mean and standard deviation SD) and Analytical: (Chi-square test, Fisher's Exact or Monte Carlo correction-test (ANOVA)).

Results

The MRI was successfully performed on 38 adult patients, including 24 (68%) men and 14 (32%) women with a mean age of 61.52 ± 10.45 year.

In our study, we found that 10 (26%) of cases had liver cirrhosis; however, 28 (73%) cases had normal liver.

In this study, we studied the effect of mass-forming CC on the liver. Additionally, we found that 11 cases (28.5%) were associated with lobar atrophy, and 27 cases (71%) were not associated with lobar atrophy.

Regarding intrahepatic biliary radicle dilatation, we found that not all cases are associated with biliary radicle dilatation. We found that 10 (26%) of cases were not associated with IHBRD, and the rest of 38 cases were associated with IHBRD varying from mild to severe.

In terms of vascular invasion, 10% of our cases showed PV invasion, whereas 5% demonstrated HA invasion.

Regarding the signal intensity of CC in DWI, a mild hyperintensity signal was detected in 11 (29%) cases,

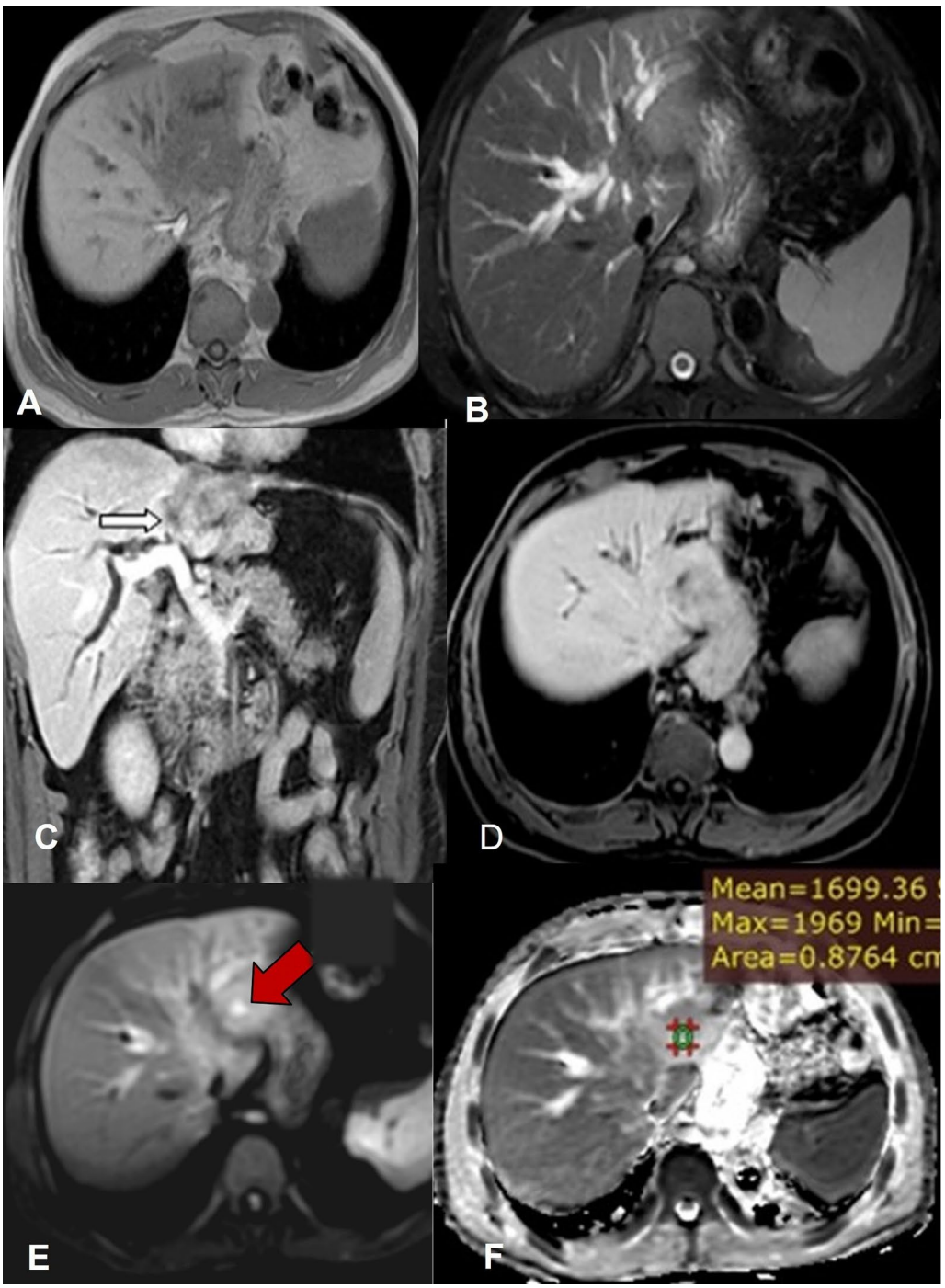

Fig. 2 A 54-year-old male patient with low-grade CC **A** axial T1WI shows a hypointense mass lesion in segments II and III of the left hepatic lobe, **B** Axial heavy T2WI shows a hyperintense mass lesion with mild intrahepatic biliary radicles dilatation **C** Coronal portovenous phase shows thrombosis left branch of portal vein, (white arrow), **D** Delayed phase shows delayed contrast retention within the lesion, **E** The lesion displays high signal intensity on DWI (restricted diffusion). **F** The ADC value of the lesion is (1.6×10^{-3} mm^2/s)

marked hyperintensity was seen in 18 (36.5%) cases, and heterogeneous intensity was detected in nine cases (23.6%).

Regarding the relation of ADC values of CC, hepatic parenchyma, and splenic parenchyma on diffusion-weighted MRI images, we found that the mean ADC

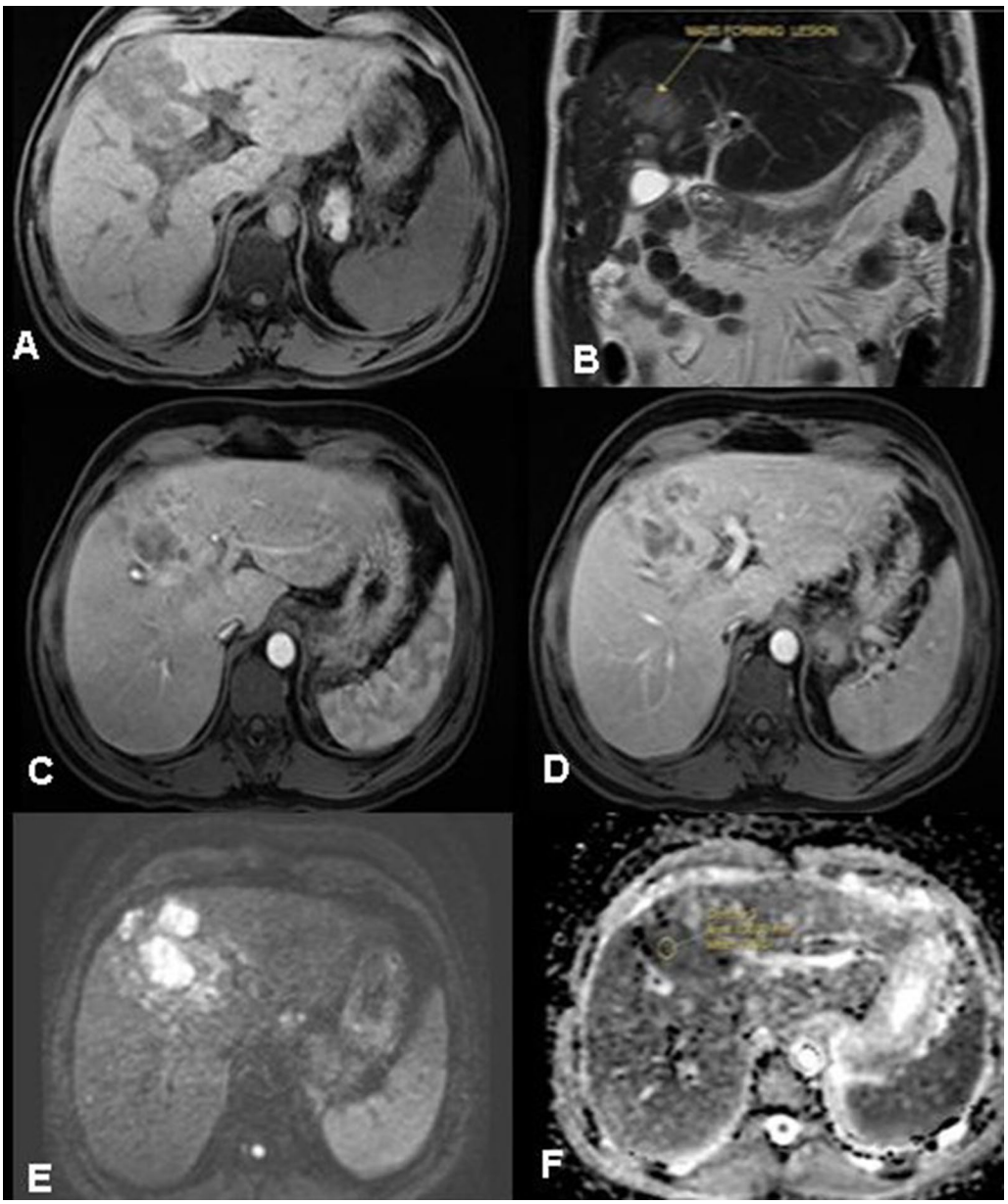

Fig. 3 A 76-year-old male patient with high-grade CC. **A** Axial T1WI shows a hypointense mass lesion in segment IV of the left hepatic lobe with subtle bulge **B** Coronal T2WI shows a hyperintense mass lesion No biliary radicles dilatation **C** Arterial phase shows heterogenous peripheral arterial enhancement of the lesion, **D** The portovenous phase shows delayed contrast retention within the lesion, **E** The lesion displays high signal intensity on DWI (restricted diffusion). **F** The ADC value of the lesion is (0.9×10^{-3} mm^2/s)

value of CC was about 1.13 ± 0.18. The mean ADC value of the normal hepatic parenchyma was 1.45 ± 0.28, and the mean ADC value of the spleen was 0.88 ± 0.17 (Table 1).

Regarding the relation between the ADC value of mass-forming CC and its pathological grading, poorly differentiated CC was associated with a lower ADC value (mean $0.98 \pm 0.12 \times 10^{-3}$ mm^2/s), while well-differentiated CC was associated with a higher ADC value (mean$1.23 \pm 0.16 \times 10^{-3}$ mm^2/s) (Table 2).

The cutoff value for poorly differentiated CC ADC measurements was less than 1.15, while it was greater than 1.15 for well-differentiated CC (Table 3).

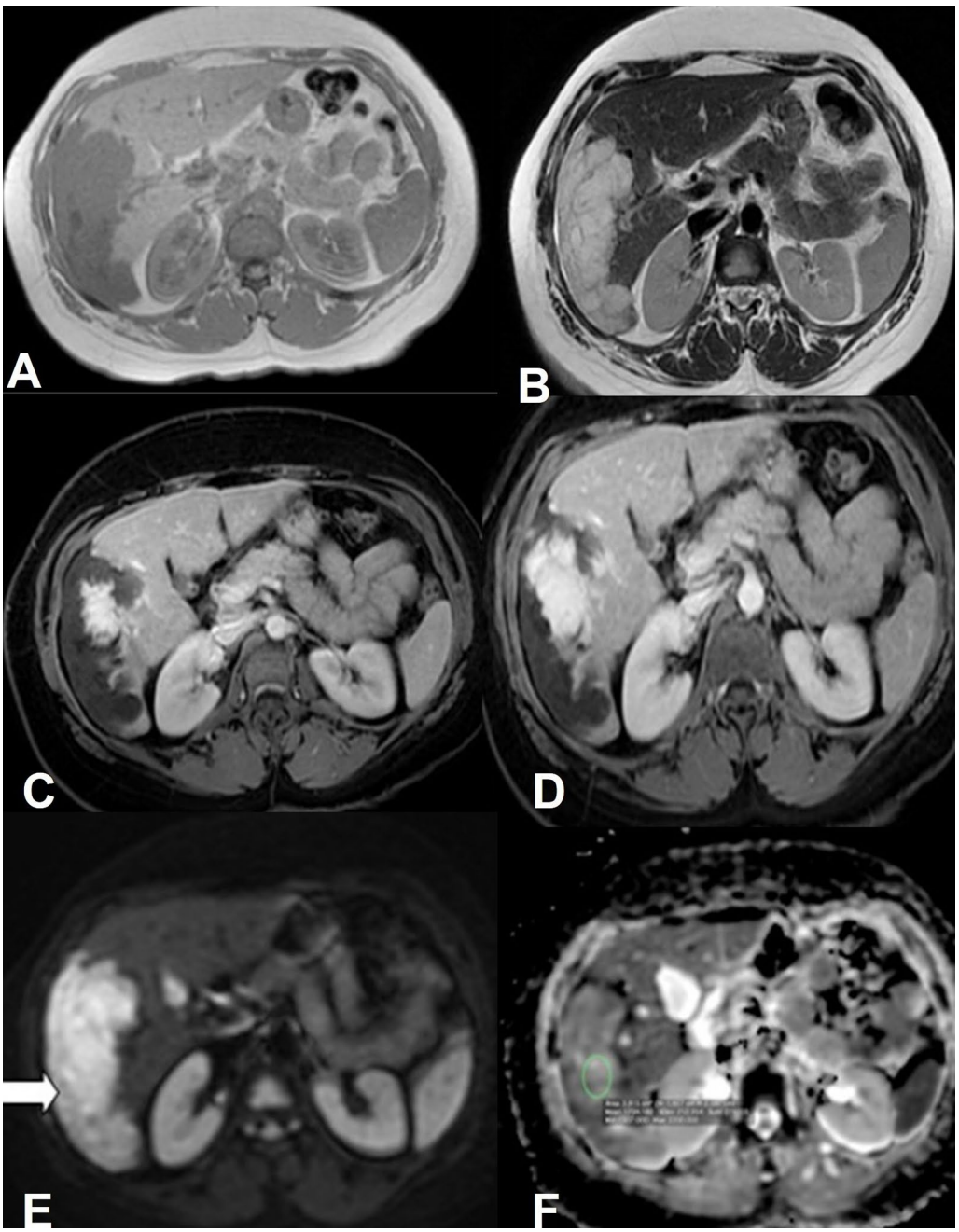

Fig. 4 A 55-year-old female patient with low-grade CC **A** axial T1WI shows a hypointense mass lesion in segments V and VI of the right hepatic lobe **B** axial T2WI shows a hyperintense mass lesion. No intrahepatic biliary radicles dilatation **C** Arterial phase shows heterogeneous arterial enhancement. **D** Delayed phase shows delayed contrast retention within the lesion. **E** The lesion displays high signal intensity on DWI (restricted diffusion). **F** The ADC value of the lesion is (1.9×10^{-3} mm^2/s)

Discussion

CC is a malignancy with various spectrums of morphophonological and prognostic characteristics [12].

Invasive and non-invasive imaging modalities are utilized for the diagnosis and staging of mass-forming CC [13]. Additional studies were conducted to evaluate new imaging techniques [13]. In this view, several researchers have suggested that diffusion-weighted (DW) MRI can contribute to increasing MRI sensitivity for mass-forming CC diagnosis [14].

DW-MRI provides a detailed picture of tissue organization, cellularity, the integrity of cells and membranes, and the tortuosity of the extracellular space, which can aid in the diagnosis of neoplastic diseases and the differentiation of neoplastic from non-neoplastic tissues [15].

In our study of 38 patients with ages ranging from 34 to 77 years, the mean age was 61.52 years, which means that CC was more predominant after the age of 60 years, which aligns with another study done by Park et al. [16] that included 52 patients with mean age 63.4 years. Regarding sex distribution, male distribution was 28 cases (73%), and female was 10 cases (26%).

In our study, we found that 10 (26%) cases had liver cirrhosis; nevertheless, 28(73%) cases had normal liver, indicating there is no strong relationship between CC and cirrhotic liver like HCC. These results were in line with Lee et al. [17], who found that the background of the liver was normal in 76 (84%) of the cases, and the remaining 15 (16%) were cirrhotic.

In this study, we investigated the effect of mass-forming CC on the liver. We found that 11 (28.5%) cases were associated with lobar atrophy, and 27 (71%) cases were not associated with lobar atrophy. This finding is consistent with Lwis et al. [18], who found that among 51 cases, 13 cases (25%) were associated with lobar atrophy and 38 cases (75%) were not associated with lobar atrophy, which was explained by the fact that CC is associated with parenchymal fibrosis which leads to lobar atrophy.

Regarding the intrahepatic biliary dilatation, we found that not all cases were associated with biliary dilatation. Furthermore, 10 (26%) cases were not associated with IHBRD, while the remaining 38 cases were associated with IHBRD varying from mild to marked. This finding is compatible with Lwis et al. [18], who found that among 51 cases, biliary dilatation was seen in 29 (57%) cases, 22 (22%) cases were not associated with biliary radicles dilatation, indicating that mass-forming CC was not always associated with biliary radicles dilatation.

With respect to vascular invasion, 10% of our cases showed PV invasion, and 5% showed HA invasion. Vascular invasion is a main-stay in the staging of CC prior to operative treatment. Comparatively, Lwis et al. [18] found that among 51 cases, 28 (45%) cases exhibited vascular invasion, and also, Lee et al. [17] found that among 91 cases, 37 cases showed vascular invasion.

Regarding the signal intensity of CC in DWI, we found that a mild hyperintensity signal was detected in 11 (29%) cases, a marked hyperintensity signal was observed in 18 (36.5%) cases, and heterogeneous intensity was found in nine cases (23.6%) of CC, indicating that the most common appearance was the marked hyperintensity. This finding is comparable to those of Lwis et al. [18], and Kovac et al. [19], who detected CC visibility at high and low B values. At high values, the most common appearance of CC was the marked hyperintensity signal, which clarified

Table 1 ADC value of cholangiocarcinoma, hepatic parenchyma and splenic parenchyma on diffusion-weighted MRI images

	ADC value for CC $N \times 10^{-3}$ mm^2/s ($n=38$)	ADC of the liver ($n=38$)	ADC of the spleen ($n=38$)
Min.–Max	0.80–1.50	0.90–2.0	0.50–1.10
Mean ± SD	1.13 ± 0.18	1.45 ± 0.28	0.88 ± 0.17
Median	1.10	1.50	0.90

ADC, apparent diffusion coefficient; SD, standard deviation; *N*, number

Table 3 The cutoff values of different mass-forming CC grades and its specificity and sensitivity

	Cutoff	Sensitivity	Specificity	PPV	NPV
Poor differentiated CC					
ADC value	**≤ 1.15**	94.44	65.38	65.4	94.4
Well-differentiated CC					
ADC value	**> 1.15**	70.83	95.0	94.4	73.1

Bold indicates cutoff value

CC, cholangiocarcinoma; ADC, apparent diffusion coefficient; PPV, positive predictive value; NPV, negative predictive value

Table 2 Relation between grading of mass-forming cholangiocarcinoma with pathological correlation and ADC value ($n=38$)

ADC value	Grading of cholangiocarcinoma with pathological correlation			*F*	*p*
	Poorly differentiated ($n=10$)	Moderately differentiated ($n=2$)	Well-differentiated ($n=26$)		
Min.–Max	0.80–1.20	1.10–1.10	1.0–1.5	16.555*	< 0.001*
Mean ± SD	0.98 ± 0.12	1.10 ± 0.0	1.23 ± 0.16		
Median	1.0	1.10	1.25		
Sig.bet.Grps	$p_1 = 0.505$, $p_2 < 0.001$*, $p_3 = 0.405$				

ADC, apparent diffusion coefficient; Sig.bet.Grps, significance between groups; SD, standard deviation; *N*, number

*Statistics significance

that restricted diffusion is a marker of dense cellularity, as observed in malignant tumors. Marked hyperintense lesions indicate marked cellularity, and heterogeneous lesions mean the highly cellular (active) areas showed restricted diffusion. In contrast, necrotic or edematous areas showed relatively free diffusion areas, providing information about tissue diffusivity and cellularity.

Regarding the comparison between the ADC value of CC and the ADC value of the liver, as well as the ADC of the spleen, we found that the ADC value of CC was lower than that of the liver and higher than that of the spleen. This finding aligns with El Fattach et al. [20], who found similar results and reported that using the spleen and the liver as reference organs was a relatively recent concept that helped improve reproducibility and reduced variability in ADC measurement. In order to accomplish this, two normalized ADC ratios were calculated for each CC. When using the normal hepatic parenchyma, measurements were facilitated when ROIs used for calculation were placed on the same slice level.

According to the relation between pathological grading of mass-forming CC and its ADC value, we found that a higher ADC value (mean$1.23 \pm 0.16 \times 10{-}3$ mm^2/s) was associated with well-differentiated CC and low ADC value (mean $0.98 \pm 0.12 \times 10{-}3$ mm^2/s) was associated with poorly differentiated CC. We also could calculate the cutoff value of well-differentiated CC ADC measurements, which was more than 1.15, whereas the cutoff value for poorly differentiated CC was less than 1.15. These results are in line with Lwis et al. [17] and Cui et al. [12], which reported that lower mean ADC values were associated with poorer tumor differentiation, which explained the value of ADC value measurement in detecting tumor degree of differentiation.

Our study has several limitations, such as using different b-value combinations, which lead to bias in ADC values. Nevertheless, we expected the bias to be relatively small. In addition, the presence of liver fibrosis or cirrhosis in many cases and the use of the liver as a reference organ when calculating the ADC values, but there was no significant difference in ADC values for livers with varying degrees of fibrosis.

Conclusions

In this study, we found that mass-forming CC had distinct qualitative MRI characteristics. Using the liver and spleen as reference organs improved reproducibility and decreased variability in ADC measurement. Poorly differentiated CC was associated with cutoff values lower than 1.15, whereas well-differentiated CC was associated with cutoff values greater than 1.15. DWI is a non-invasive, simple, non-contrast-dependent technique that aids in the diagnosis and grade differentiation of mass-forming CC.

Abbreviations

ADC: Apparent diffusion coefficient; DWI: Diffusion-weighted imaging; CC: Cholangiocarcinoma; IHBRD: Intrahepatic biliary radicle dilatation; MRI: Magnetic resonance imaging; US: Ultrasonography; MDCT: Multi-detector computed tomography; SE-EPI: Spin-echo echo-planar imaging; GD: Gadolinium; SD: Standard deviation.

Acknowledgements

Not Applicable.

Author contributions

HAS contributed to writing the research, sharing in selection of the cases; sharing in figures preparation of cases. MRE contributed to sharing in cases selection and review. TFA shared in cases selection and review. MSA carried out cases on workstation and selection of research cases, prepared the figures for cases demonstration, writing and review of the research. "All authors read and approved the final manuscript."

Funding

This study had no funding from any resource.

Availability of data and materials

The datasets used and/or analyzed during the current study are available from the corresponding author on reasonable request.

Declarations

Ethics approval and consent to participate

All procedures followed were in accordance with the ethical standards of the responsible committee on human experimentation (Institutional Review Board (IRB)" of National Liver Institute Menoufia University and with the Helsinki Declaration of 1964 and later versions. Committee's reference number is unavailable (NOT applicable). No consent was obtained from the patients since it was a retrospective study.

Consent for publication

All patients included in this research gave written informed consent to publish the data contained within this study.

Competing interests

The authors declare that they have no competing interests.

Author details

[1]Radiology Department, National Liver Institute, El-Menofuia University, Shebin Elkoum, Egypt. [2]Radiology Department, Faculty of Medicine, Menoufia University, Shebin Elkoum, Egypt.

Received: 17 June 2022 Accepted: 10 November 2022
Published online: 23 November 2022

References

1. Chandarana H, Taouli B (2010) Diffusion and perfusion imaging of the liver. Eur J Radiol 76(3):348–358
2. Taouli B (2012) Diffusion-weighted MR imaging for liver lesion characterization: acritical look. Radiology 262(2):378–380
3. Jarnagin WR (2000) Cholangiocarcinoma of the extrahepatic bile ducts. SemiNSurgOncol 19:156–176
4. Ganeshan D, Moron FE, Szklaruk J (2012) Extrahepatic biliary cancer: new staging classification. World J Radiol 4:345–352
5. Nagorney DM, Donohue JH, Farnell MB et al (1993) Outcomes after curative resections of cholangiocarcinoma. Arch Surg 128(8):871–878
6. Manfredi R, Barbaro B, Masselli G et al (2004) Magnetic resonance imaging of cholangiocarcinoma. Semin Liver Dis 24:155–164

7. Soyer P, Bluemke DA, Hruban RH et al (1994) Primary malignant neoplasms of the liver: detection with helical CT during arterial portography. Radiology 192:389–392
8. Choi B, Lee J, Han J (2004) Imaging of intrahepatic and hilar cholangiocarcinoma. Abdom Imaging 29(5):548–557
9. Ahrendt SA, Nakeeb A, Pitt HA (2001) Cholangiocarcinoma. Clin Liver Dis 5:191–218
10. Jhaveri KS, Hosseini-Nik H (2015) MRI of cholangiocarcinoma. J Magn Reson Imaging 42:1165–1179
11. Gangahdar K, Santhosh D, Chintapalli KN (2014) MRI evaluation of masses in the noncirrhotic liver. Appl Radiol 43:20–28
12. Della Corte A, Di Gaeta E, Steidler S (2022) Radiological imaging and non-surgical local treatments for cholangiocarcinoma. Hepatoma RES 8:2454–2469
13. Cui XY, Chen HW (2010) Role of diffusion-weighted magnetic resonance imaging in the diagnosis of extra-hepatic cholangiocarcinoma. World J Gastroenterol 16(25):3196–3201
14. Sainani NI, Catalano OA, Holalkere NS et al (2008) Cholangiocarcinoma: current and novel imaging techniques. Radiographics 28(5):1263–1287
15. Aljiffry M, Walsh MJ, Molinari M (2009) Advances in diagnosis, treatment and palliation of cholangiocarcinoma: 1990–2009. World J Gastroenterol 15:4240–4262
16. Park HJ, Kim SH, Jang KM et al (2014) The role of diffusion-weighted MR imaging for differentiating benign from malignant bile duct strictures. Eur Radiol 24(4):947–958
17. Lee J, Kim SH, Kang TW et al (2016) Mass-forming intrahepatic cholangiocarcinoma: diffusion-weighted imaging as a preoperative prognostic marker. Radiology 281:119–128
18. Lwis S, Besa C, Wagner M et al (2018) Prediction of the histopathological finding of the intrahepatic cholangiocarcinoma: qualitative and quantitave assessment of diffusion—weighted imaging. EurRadiol 28(5):2047–2057
19. Kovac JD, Jankovic A, Đikic-Rom A et al (2022) Imaging spectrum of intrahepatic mass-forming cholangiocarcinoma and its mimickers: how to differentiate them using MRI. Curr Oncol 29:698–723
20. El Fattach H, Dohan A, Guerrache Y, Dautry R et al (2015) Intrahepatic and hilar mass-forming cholangiocarcinoma: qualitative and quantitative evaluation with diffusion-weighted MR imaging. Eur J Radiol 84(8):1444–1451

Publisher's Note